

The Study of Demagnetization of the Magnetic Orientation of Permanent Magnets for IPMSM with Field-Weakening Control under Hot Temperature

Noriyoshi Nishiyama¹, Hiroki Uemura² and Yukio Honda²

1. *Panasonic Corporation, Moriguchi City, Osaka 570-8501, Japan*

2. *Osaka Institute of Technology, Osaka City, Osaka 530-0013, Japan*

Abstract: In this study, we investigate the demagnetization resistance of a concentrated winding IPMSM (interior permanent magnet synchronous motor) accounting for field weakening control by changing the magnetization direction of the permanent magnet under a high-temperature environment. IPMSMs are investigated by FEA (finite element analysis) using the same volume of the permanent magnet while changing the magnet's width, thickness and magnetic field orientation angle. FEA found that a V-shaped angle $V_a = 100^\circ$ and a changed magnet length of 97% using an oblique magnetic-field-oriented magnet strike a good balance between demagnetization resistance and torque at 180 °C. Comparison between demagnetization of negative d-axis current (current phase $\beta = 90^\circ$) and demagnetization of field weakening control ($\beta = 80^\circ$) using concentrated winding IPMSM with V-shaped angle $V_a = 100^\circ$ is conducted. With the demagnetization factor at $\beta = 80^\circ$ for $\beta = 90^\circ$, the demagnetization factor 0.39 (2.6 times) at $\alpha = 0^\circ$ decreases to 0.23 (4.3 times) at $\alpha = 20^\circ$. The demagnetization resistance in the field weakening control is further improved.

Key words: IPMSM, demagnetization, concentrated winding, high temperature, field weakening.

1. Introduction

The high efficiency of a small-sized permanent magnet synchronous motor is one of its key features. On the other hand, one of its disadvantages is that the coercive force decreases at high temperature and then easily demagnetizes. In recent years, motors for vehicles, high-temperature heat pumps, and extreme-environment-compatible robots have had to operate in severe load environments, which are often extremely high-temperature environments where permanent magnets are demagnetized. In this work, we examined a parallelogram-shaped permanent magnet whose magnetic field orientation was made oblique with respect to the plate thickness direction (see Fig. 1). L_m is the magnet length, A_m is the magnet cross-sectional area.

Corresponding author: Noriyoshi Nishiyama, doctor of philosophy in Engineering, research fields: permanent magnet synchronous motor design.

For obliquely distributed magnets with an oblique orientation angle α , the magnetic field orientation inclines from the plate thickness direction with respect to the magnet width W_m and the magnet thickness t_m . Furthermore, the operating point of the magnet does not change much from the permeance equation, since the magnetic field H is acting on the magnet. On the other hand, the reverse magnetic field component affecting the magnetization direction of the magnet can be reduced to H_m , thus improving the demagnetization resistance [1, 2].

Few studies have attempted to examine the magnetic field orientation of permanent magnets detailed demagnetization characteristics under high temperature environments [3-8]. A field weakening control that energizes the negative d-axis current component can suppress the induced voltage of the motor and can operate in the wide rotational speed range under a limited power supply voltage [9]. The demagnetization in field-weakening control is likely to

Magnetic field orientation angle

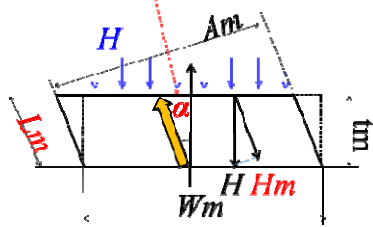


Fig. 1 Oblique magnetic oriented magnet.

occur at a current phase $\beta = 80^\circ$ where the negative d-axis current component is very large.

In this paper, we investigate the optimum design for improving the demagnetization resistance of a concentrated winding IPMSM (interior permanent magnet synchronous motor) accounting for field weakening control by changing the magnetization direction of the permanent magnet under a high-temperature environment.

2. Demagnetization Analysis

A concentrated winding motor is advantageous for use in high-temperature environments. In addition, IPMSM, in which a magnet is embedded in a rotor core, is generally arranged in a rectangular parallelepiped permanent magnet, and by deeply embedding a magnet in the rotor core, the magnetic field acting on the magnet can be relaxed, which improves the demagnetization resistance.

Permeance coefficient P_c , which determines the operating point of the permanent magnet, is expressed as Eq. (1):

$$P_c = \frac{LmAg}{AmLg} \sigma f \quad (1)$$

where Ag is the air across-sectional area, Lg is the air gap length, σ is the leak coefficient, and f is the magneto motive force loss factor.

The improvement of the demagnetization resistance is greatly affected by the angle difference between the direction of the working magnetic field and the magnet orientation direction. The aim of demagnetization analysis is to study the optimum design by changing the magnetic field orientation angle α and the magnet

arrangement angle V_a while also changing the magnet length Lm and magnet width Wm under a fixed magnet volume at 180 °C. A current causing a reverse magnetic field to act on the rotor's magnet is passed through the winding and the air gap, and magnetic flux density before and after energy conduction is obtained by electromagnetic field analysis software (JMAG-Designer). A neodymium sintered magnet (reversible data of NMX-S 36 UH) is used. [10]

The analysis conditions are shown in Table 1, and the analysis model is shown in Fig. 2. The evaluation indexes are demagnetization limit current and torque.

The demagnetization ratio $Dr n$ is defined as Eq. (2): The demagnetization improvement ratio $Dir n$ is defined as Eq. (3):

$$Dr n = 100 \times (1 - B2/B1) \quad (2)$$

$$Dir n = Dr n / Dr 0 \quad (3)$$

The torque ratio $Tr n$ is defined as Eq. (4):

$$Tr n = T n / T 0 \quad (4)$$

where $B1$ is the air gap's magnetic flux density before reversed magnetic field is applied. $B2$ is the air gap's magnetic flux density after reversed magnetic field is applied. $Dr 0$ is the demagnetization ratio at the

Table 1 Analysis conditions.

Stator ID	56 mm	Residual magnetic flux density Br	1.16 T
Rotor OD	54.4 mm	Coercivity Hcj	2,387 kA/m
Stack length	32 mm	Electromagnetic steel sheet	35A300
Magnet	1135 mm ³ (at one pole)	Temperature	180 °C
Winding	150 turn, 3Y		

Magnet arrangement angle $V_a = 60^\circ \sim 180^\circ$

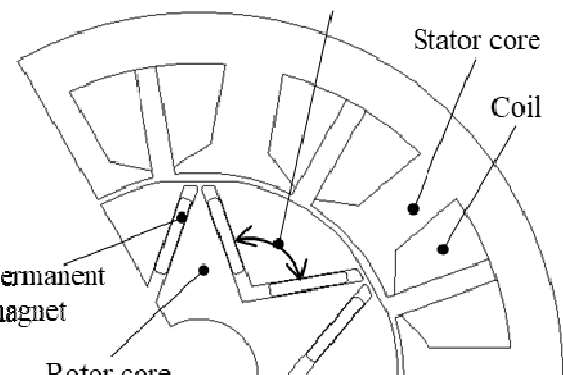


Fig. 2 V-shaped magnet arrangement motor model.

parallel-oriented magnet ($\alpha = 0^\circ$) placed in flat arrangement ($V_a = 180^\circ$). T_0 is the torque at the parallel-oriented magnet ($\alpha = 0^\circ$) placed in flat arrangement ($V_a = 180^\circ$).

The demagnetization limit current is the maximum current at which reduction of the non-conducting air gap's magnetic flux density, before and after application of the reverse magnetic field current, does not yet reach 1%.

The torque is calculated with rated current (7.07 Arms) and current phase $\beta = 20^\circ$.

3. Magnet Length and Demagnetization Resistance

Here, we consider demagnetization analysis by an analytical model in which the magnet arrangement angle V_a is changed from 180° to 60° .

Based on a 1% demagnetization limit current of the flat plate model ($V_a = 180^\circ$), this value is increased 3 times for the $V_a = 100^\circ$ model and 8 times for the spoke model ($V_a = 60^\circ$). As the magnet arrangement angle V_a is changed, demagnetization improvement ratio Dr_n and torque ratio Tr_n are in a trade-off relationship (see Fig. 3).

In the analysis results, the horizontal axis shows the magnet length ratio and the vertical axis shows the demagnetization resistance improvement ratio or the torque ratio (see Figs. 4 and 5).

For the demagnetization resistance improvement ratio, the demagnetization limit current of a rotor with the flat-plate magnet arrangement using a parallel-oriented magnet is 100% (circle within solid line; 1). The torque ratio is the ratio of the parallel-oriented magnets to the flat arrangement rotor's torque (circle within solid line; 1). Under the condition of a constant magnet volume, at a magnet length of less than 100%, the magnet width is increased. On the other hand, at a magnet length of 100% or more, the magnet width is constant using an oblique magnetic-field-oriented magnet.

Although the demagnetization improvement ratio

increases in the V-shaped arrangement, the demagnetization improvement ratio also decreases as the magnet length ratio decreases. Further, if the

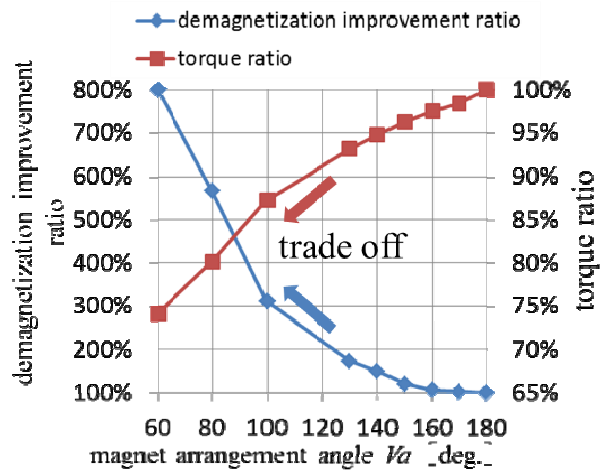


Fig. 3 Magnet arrangement angle V_a vs. demagnetization ratio and torque ratio.

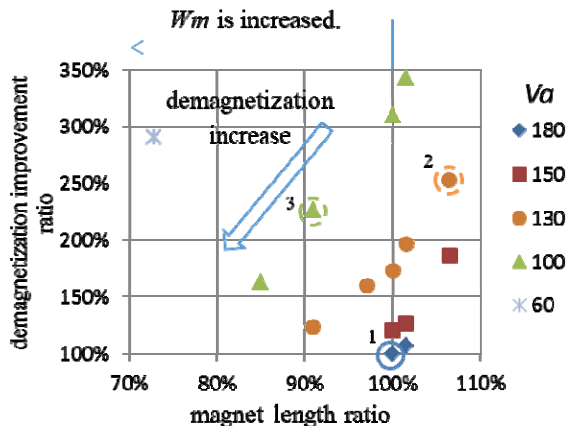


Fig. 4 Magnet length ratio vs. demagnetization improvement ratio.

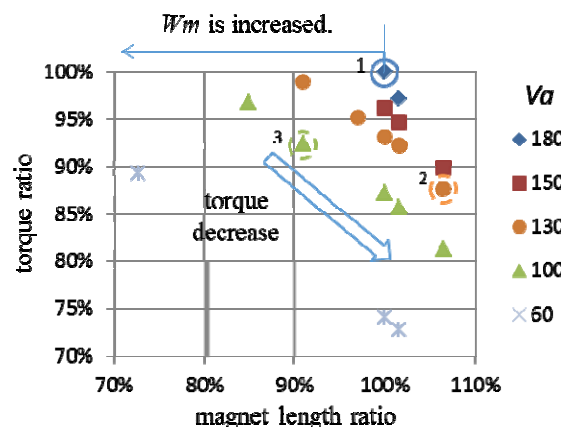


Fig. 5 Magnet length ratio vs. torque ratio

demagnetization improvement ratio is improved, the torque ratio decreases. Aiming for demagnetization improvement ratio of 200% or more, the torque ratio becomes 90% or less (circle in dotted line; 2.3). They are in a trade-off relationship.

Next, we investigate the possibility of improving the demagnetization resistance by oblique magnetic field oriented magnets when the magnet length ratio of $V_a = 100^\circ$ model is less than 100%.

In the oblique magnetic-field-oriented magnet, even if the magnet thickness tm is small, the magnet length Lm can be increased, and thus improvement in demagnetization resistance can be expected. Using the $V_a = 100^\circ$ model offers a lot of latitude in the magnet arrangement, so we investigated the demagnetization resistance and torque using the magnet length Lm as a parameter.

A list of the studied magnets is given in Table 2, based on a motor model in which magnet 1 is used as a reference. Demagnetization is evaluated as the ratio of the demagnetization limit current ratio to the 1% demagnetization limit current. Torque is evaluated as the ratio of the magnet's torque ratio to the average value of the air gap's magnetic flux density at the time of non-conduction. The torque of the IPMSM is the sum of the magnet torque and the reluctance torque, since the maximum torque per current is about 20° in the current phase and this is a motor model mainly based on magnet torque. In order to clarify the influence of using different magnets, here we compare the torque with the magnet torque ratio.

In the analysis results (see Fig. 6), the horizontal axis is the magnet length ratio, and the vertical axis shows the demagnetization limit current ratio and the torque ratio. The demagnetization limit current ratio is greatly reduced for a motor using magnet 2 or magnet 3 with a magnetic field orientation angle $\alpha = 0^\circ$ obtained by increasing the magnetic width Wm through reducing the magnet thickness tm (i.e., reduction of the magnet length Lm).

On the other hand, in a motor in which magnet 4 or

Table 2 Magnet parameters.

No.	Magnet length Lm [mm]	Magnet width Wm [mm]	magnetic orientation angle α [deg.]	magnet length ratio
1	1.65	10.75	0	100%
2	1.60	11.1	0	97%
3	1.50	11.8	0	91%
4	1.50	11.8	20	97%
5	1.40	12.7	20	90%

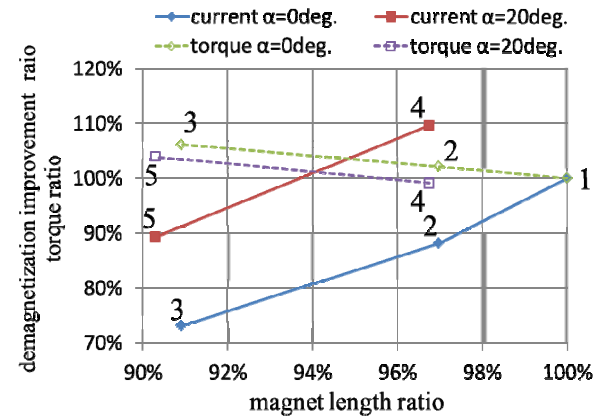


Fig. 6 Magnet length ratio vs. demagnetization improvement ratio.

magnet 5 with the magnetic field orientation angle $\alpha = 20^\circ$ is used, the demagnetization limit current ratio is improved over that of the motor using magnets with the magnetic field orientation angle $\alpha = 0^\circ$. The change in the torque ratio increases as the magnet width Wm increases, but it is smaller than the change in the demagnetization limit current ratio.

4. Demagnetization Ratio at Field-Weakening Control

The demagnetization ratio of the field weakening control ($\beta = 80^\circ$) decreases with respect to the negative d-axis of the current ($\beta = 90^\circ$), and this ratio is defined as the current phase demagnetization ratio $Cr n$.

$$Cr 80 = Dr 80 / Dr 90 \quad (5)$$

where, $Dr 80$ is the demagnetization ratio at $\beta = 80^\circ$, $Dr 90$ is the demagnetization ratio at $\beta = 90^\circ$.

The smaller the current phase demagnetization ratio Cr , the more margin is given to the demagnetization resistance in the field-weakening control.

Fig. 7 shows the relationship between the demagnetization ratio Dr with respect to the current at the magnetic orientation angle $\alpha = 0^\circ$ and $\alpha = 20^\circ$ in the $V_a = 130^\circ$ model. At the magnetic orientation angle $\alpha = 0^\circ$, when the current is 42.5 A, the demagnetization ratio at $\beta = 90^\circ$ (Dr 90) is 0.91%, and the demagnetization ratio at $\beta = 80^\circ$ (Dr 80) is 0.79%. When the current phase differs by 10° , the demagnetization ratio is reduced to 0.87 times.

At the magnetic orientation angle $\alpha = 20^\circ$, when the current is 70 A, the demagnetization ratio at $\beta = 90^\circ$ (Dr 90) is 0.91%, and the demagnetization ratio at $\beta = 80^\circ$ (Dr 80) is 0.67%. If the current phase differs by 10° , the demagnetization factor is reduced to 0.67 times.

At $\alpha = 20^\circ$ with respect to $\alpha = 0^\circ$, in addition to the large demagnetizing resistance current, the demagnetization ratio when β is shifted from 90° to 80° is small, the demagnetization resistance ratio is high.

5. Magnet Length and Demagnetization Ratio at Field Weakening Control

Fig. 8 shows the current phase demagnetization ratio Cr with respect to the magnet length ratio, which is 1, 2, 3, 4, and 5 in Table 2. With the magnetic field orientation angle $\alpha = 0^\circ$, the motor using magnet 1 (magnet length 100%) indicates $Cr = 0.39$. With the magnet length ratio of 97%, the motor using magnet 2 indicates $Cr = 0.34$. On the other hand, with the magnetic field orientation angle $\alpha = 20^\circ$, the motor using magnet 4 indicates a smaller $Cr = 0.23$. With the magnet length ratio of 90% and, the magnetic field orientation angle $\alpha = 0^\circ$, the motor using the magnet 3 indicates $Cr = 0.54$; whereas with the magnet orientation angle $\alpha = 20^\circ$, the motor using magnet 5 indicates a smaller $Cr = 0.44$.

At the magnet length ratio of 97% (magnet 2, magnet 4), the current phase demagnetization ratio Cr is improved. At the magnet length ratio of 90%, Cr is as low as 74% (magnet 3), and at demagnetization

improvement ratio $Dir = 90\%$ (magnet 5), Cr is about the same value as magnet 1.

At the demagnetization improvement ratio $Dir = 90\%$ or more, the current phase demagnetization ratio Cr is also improved.

6. Measurement of Magnetic Flux Density

We evaluate the magnetic flux density of prototype magnets with oblique orientation. The prototype magnets were produced by obliquely slicing samarium cobalt sintered magnet with respect to the magnetic field orientation direction. Since there is a large market demand for neodymium sintered magnets, it is difficult to use them for special prototypes under development; therefore, we used samarium cobalt sintered magnets to evaluate the difference in orientation angles.

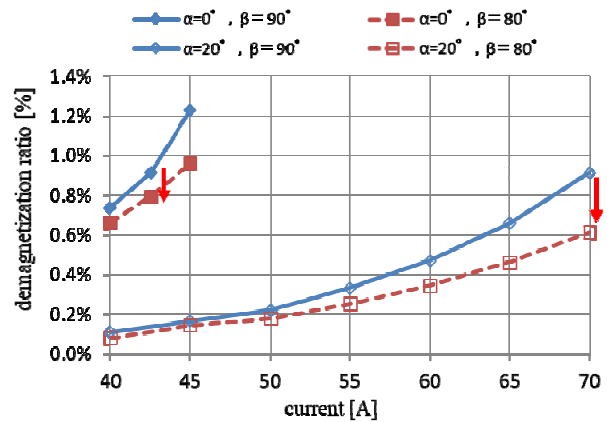


Fig. 7 Current vs. demagnetization ratio.

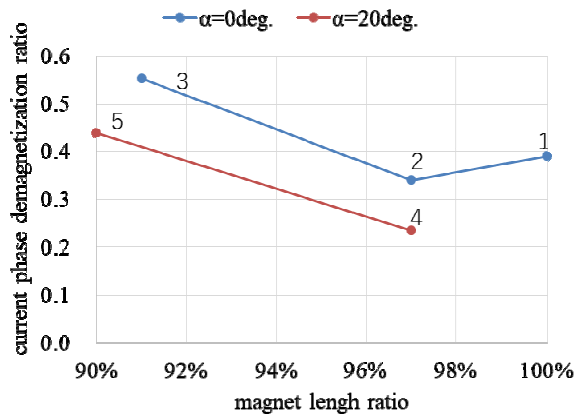


Fig. 8 Magnet length ratio vs. current phase demagnetization ratio.

Two types of magnets have the following magnetic field orientation angles: $\alpha = 0^\circ, 20^\circ$. The prototype magnet size is magnet thickness $tm = 1.8$ mm, magnet width $Wm = 10.8$ mm, and axial length $L = 31$ mm. The magnetic flux density measuring device is composed of a magnet analyzer (MAD-300R, DMT), a tesla meter (TM-4700, DMT), and an ultrafine probe (w 0.75 mm - t 0.28 mm F-075, DMT) with a resolution of 21,600 (see Fig. 9).

Next, the prototype magnets were assembled into a rotor with magnet arrangement angle $Va = 130^\circ$, and the magnetic flux density was measured. Furthermore, the rotor was assembled in a cylindrical dummy stator made of a magnetic body having the same inner diameter as the stator core, and the magnetic flux density of the air gap was measured (see Fig. 10).

We discuss the results of the air gap's magnetic flux density measured for the rotor assembled in the dummy stator. As a result of measuring the air gap's magnetic flux density, it is found that the maximum magnetic field orientation angle decreased slightly, but the magnetic flux density distribution approached a sinusoidal wave form and is thus effective for reducing the torque ripple.

Fig. 11 shows the air gap magnetic flux density of the motor by FEA. The magnetic field orientation angle $\alpha = 0^\circ$ indicated by the solid line and $\alpha = 20^\circ$ indicated by the broken line are non-energized air gap magnetic flux densities.

The magnetic flux density of 47° to 53° and 87° to

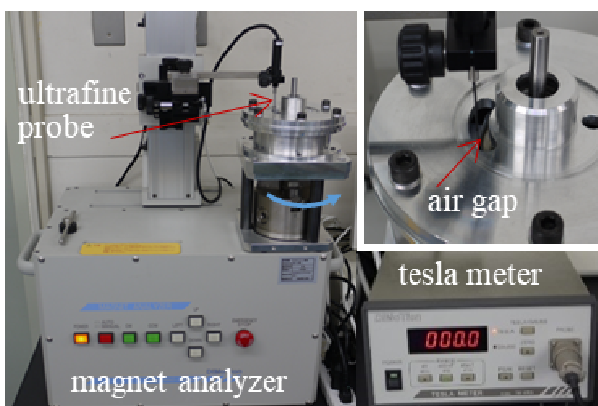


Fig. 9 Air gap magnet flux density measuring device.

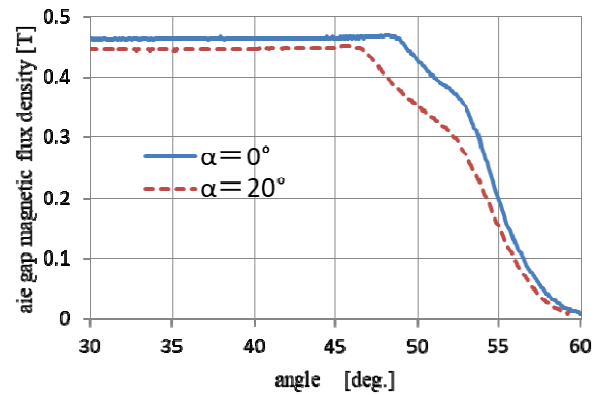


Fig. 10 Air gap magnet flux density (measured).

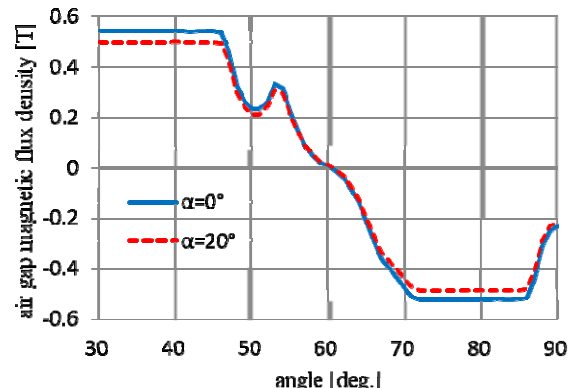


Fig. 11 Air gap magnet flux density (analysis).

90° on the horizontal axis is distorted by the open slot of the stator. The air gap magnetic flux density of $\alpha = 20^\circ$ is as small as 7% as compared with $\alpha = 0^\circ$, close to a sinusoidal wave from 66° to 72° on the horizontal axis without the effect of open slot. It is similar to the actual measurement at the air gap magnetic flux density of the cylinder dummy stator.

7. Conclusions

In this paper, we examined the optimum design accounting for field-weakening control oblique magnetic field orientation of IPMSM driven under a high-temperature environment, changing the magnet thickness tm and magnet width Wm while maintaining a constant magnet volume. We obtained that the demagnetization factor Cr at $\beta = 80^\circ$ for $\beta = 90^\circ$, $Cr = 0.39$ (2.6 times) at $\alpha = 0^\circ$ decreases to $Cr = 0.23$ (4.3 times) at $\alpha = 20^\circ$ by FEA (finite element analysis) and investigation of our prototype. The demagnetization

resistance of the oblique magnetic orientation magnets IPMSM in the field-weakening control is further improved.

References

- [1] Nishiyama, N., and Honda, Y. 2016. "Development of IPMSM for High Temperature Conditions Using Inclined Magnetic Field Orientation and V-Shape Magnet Arrangement." In *Proceedings of IEEJ Joint Technical Meeting on "Magnetics" and "Linear Drives" MAG-16-2010, LD-16-145*, pp. 23-8. (in Japanese)
- [2] Uemura, H., Nishiyama, N., and Honda, Y. 2017. "The Effeteness of Magnetic field directions of V shaped embedded magnets for IPMSM." In *Proceedings of 2017 Ann. Meet. Rec. IEEJ, V*, p. 15. (in Japanese)
- [3] Nishiyama, N., Uemura, H., and Honda, Y. 2017. "The Study of Highly Demagnetization Performance IPMSM under Hot Environments." In *International Conference on Electrical Machines and Systems 2017 Proceedings*, 8056505.
- [4] Asano, Y., Honda, Y., Takeda, Y., and Morimoto, S. 2001. "Reduction of Vibration on Concentrated Winding Permanent Magnet Synchronous Motors with Considering Radial Stress." *IEEJ Trans. on Ind. Appl.* I21 (11): 1185-91. (in Japanese)
- [5] Maeda, Y., Urata, S., and Nakai, H. 2016. "The Evaluation of Demagnetizing Characteristics of the Permanent Magnet in Arbitrary Directions." In *Proceedings of 2016 Ann. Meet. Rec. IEEJ, II*, pp. 124-5. (in Japanese)
- [6] Akune, R., Akatsu, K., Kume, K., Yamamoto, T., and Saito, S. 2016. "The Anti Demagnetization Method for Permanent Magnet Synchronous Motor Focused on Magnetized Direction of Permanent Magnet and Basic Experiment." In *2016 IEE-Japan Industry Applications Society Conference (JIASC2016)*, 3-54. (in Japanese)
- [7] Peng, P., Xiong, H., Zhang, J., Li, W., Leonardi, F., Rong, C., Degner, M. W., Liang, F., and Zhu, L. 2016. "Effects of External Field Orientation on Permanent Magnet Demagnetization." In *Proceedings of IEEE Energy Conversion Congress and Exposition 2016*, 7855067.
- [8] Galea, M., Papini, L., Zhang, H., Gerada, C., and Hamiti, T. 2015. "Demagnetization Analysis for Halbach Array Configurations in Electrical Machines." *IEEE Trans. on Magn.* 51 (9): 8107309.
- [9] Kawano, S., Murakami, H., Nishiyama, N., Ikkai, Y., Honda, Y., and Higaki, T. 1997. "High Performance Design of an Interior Permanent Magnet Synchronous Reluctance Motor for Electric Vehicles." In *Proceedings of Power Conversion Conference*, Nagaoka, Vol. 1, pp. 33-6.
- [10] Nishiyama, N., Uemura, H., and Honda, Y. 2017. "The Optimum Design of the Magnetic Orientation of Permanent Magnets for IPMSM under Hot Environments." In *Proceedings of IEEE International Conference on Power Electronics and Drive Systems*, pp. 380-5.